Molecular Pharmacology Fast Forward. Published on May 1, 2020 as DOI: 10.1124/mol.119.118844
This article has not been copyedited and formatted. The final version may differ from this version.

MOL #118844

TMEM16A Ca^{2+}-activated Cl^- channel regulates the proliferation and migration of brain capillary endothelial cells

Takahisa Suzuki, Miki Yasumoto, Yoshiaki Suzuki, Kiyofumi Asai,

Yuji Imaizumi, and Hisao Yamamura

Department of Molecular and Cellular Pharmacology, Graduate School of Pharmaceutical Sciences, Nagoya City University, Nagoya 467-8603, Japan (T.S., M.Y., Y.S., Y.I., H.Y.);

Department of Molecular Neurobiology, Graduate School of Medical Sciences, Nagoya City University, Nagoya 467-8601, Japan (K.A.)

Molecular Pharmacology Fast Forward. Published on May 1, 2020 as DOI: 10.1124/mol.119.118844
This article has not been copyedited and formatted. The final version may differ from this version.

MOL #118844

Running title: TMEM16A channels in vascular endothelial cells

Corresponding author:

Hisao Yamamura, Ph.D.

Department of Molecular and Cellular Pharmacology

Graduate School of Pharmaceutical Sciences

Nagoya City University

3-1 Tanabedori, Mizuhoku, Nagoya 467-8603, Japan

Tel./Fax: +81-52-836-3431

E-mail: yamamura@phar.nagoya-cu.ac.jp

Number of text page: 37

Number of tables: 0

Number of figures: 8

Number of references: 39

Number of words in the Abstract: 242

Number of words in the Introduction: 568

Number of words in the Discussion: 1378

Molecular Pharmacology Fast Forward. Published on May 1, 2020 as DOI: 10.1124/mol.119.118844
This article has not been copyedited and formatted. The final version may differ from this version.

Abbreviations: BBB, blood-brain barrier; BCEC, brain capillary endothelial cell; BK_{Ca}, large-conductance Ca^{2+}-activated K^+; BrdU, bromodeoxyuridine; $[Ca^{2+}]_{cyt}$, cytosolic Ca^{2+} concentration; Cl_{Ca}, Ca^{2+}-activated Cl^-; DMEM, Dulbecco's modified Eagle's medium; EGTA, *O,O'*-bis(2-aminoethyl)ethyleneglycol-*N,N,N',N'*-tetraacetic acid; FBS, fetal bovine serum; fura-2/AM, fura-2 acetoxymethyl ester; GAPDH, glyceraldehyde-3-phosphate dehydrogenase; GFAP, glia fibrillary acidic protein; HEK, human embryonic kidney; HEPES, 2-[4-(2-hydroxyethyl)-1-piperazinyl]ethanesulfonic acid; ICC, interstitial cells of Cajal; K_{IR}, inward-rectifying K^+; mBCEC, mouse brain capillary endothelial cell; MTT, 3-(4,5-dimethyl-2-thiazolyl)-2,5-diphenyl-2H-tetrazolium bromide; NFA, niflumic acid; PBS, phosphate-buffered saline; PCR, polymerase chain reaction; PDGFR-β, platelet-derived growth factor receptor-β; SDS-PAGE, sodium dodecyl sulfate-polyacrylamide gel electrophoresis; siRNA, small-interfering RNA; SK_{Ca}, small-conductance Ca^{2+}-activated K^+; TEA, tetraethylammonium; STIM, stromal interaction molecule; TEER, trans-endothelial electrical resistance; TRP, transient receptor potential; TRPC, transient receptor potential canonical subfamily; τ_{act}, time constant for current activation; τ_{deact}, time constant for current deactivation.

Molecular Pharmacology Fast Forward. Published on May 1, 2020 as DOI: 10.1124/mol.119.118844
This article has not been copyedited and formatted. The final version may differ from this version.

Abstract

The blood-brain barrier (BBB) is essential for the maintenance of homeostasis in the brain. Brain capillary endothelial cells (BCECs) comprise the BBB, and thus a delicate balance between their proliferation and death is required. Although the activity of ion channels in BCECs is involved in BBB functions, the underlying molecular mechanisms remain unclear. In the present study, the molecular components of Ca^{2+}-activated Cl^- (Cl_{Ca}) channels and their physiological roles were examined using mouse BCECs (mBCECs) and a cell line derived from bovine BCECs, t-BBEC117. Expression analyses revealed that TMEM16A was strongly expressed in mBCECs and t-BBEC117 cells. In t-BBEC117 cells, whole-cell Cl^- currents were sensitive to the Cl_{Ca} channel blockers, 100 μM niflumic acid and 10 μM $T16A_{inh}$-A01, and were also reduced markedly by small-interfering RNA (siRNA) knockdown of TMEM16A. Importantly, block of Cl_{Ca} currents with Cl_{Ca} channel blockers or TMEM16A siRNA induced membrane hyperpolarization. Moreover, treatment with TMEM16A siRNA caused an increase in resting cytosolic Ca^{2+} concentration ($[Ca^{2+}]_{cyt}$). $T16A_{inh}$-A01 reduced cell viability in a concentration-dependent manner. Either Cl_{Ca} channel blockers or TMEM16A siRNA also curtailed cell proliferation and migration. Furthermore, Cl_{Ca} channel blockers attenuated the trans-endothelial permeability. In combination, these results strongly suggest that TMEM16A contributes to Cl_{Ca} channel conductance and can regulate both the resting membrane potential and $[Ca^{2+}]_{cyt}$ in BCECs. Our data also reveals how these BCECs may be involved in the maintenance of BBB functions, since both the proliferation and migration are altered following changes in channel activity.

Molecular Pharmacology Fast Forward. Published on May 1, 2020 as DOI: 10.1124/mol.119.118844
This article has not been copyedited and formatted. The final version may differ from this version.

Significance Statement

In brain capillary endothelial cells (BCECs) of the blood-brain barrier (BBB), TMEM16A is responsible for Ca^{2+}-activated Cl^- channels and can regulate both the resting membrane potential and cytosolic Ca^{2+} concentration, contributing to the proliferation and migration of BCECs. The present study provides novel information on the molecular mechanisms underlying the physiological functions of BCECs in the BBB and a novel target for therapeutic drugs for disorders associated with dysfunctions in the BBB.

Molecular Pharmacology Fast Forward. Published on May 1, 2020 as DOI: 10.1124/mol.119.118844
This article has not been copyedited and formatted. The final version may differ from this version.

Introduction

The blood-brain barrier (BBB) plays a critical role in the regulation of homeostasis in the brain microenvironment. Under physiological conditions, the BBB restricts the movement of substances between the circulation and the brain, and protects neurons from the invasion of peripheral noxious substances. The BBB is formed by brain capillary endothelial cells (BCECs). BCECs are structurally characterized by intercellular tight junctions, relatively low transcellular transport activity, and surrounding cell types including pericytes, astrocytes, neurons, and microglia. These surrounding cells form a neurovascular unit, which contributes to the maintenance and enhancement of the BBB (Abbott et al., 2006; Nakagawa et al., 2009). The barrier function of the BBB is maintained by the turnover of BCECs, and these involves a dynamic balance between the production of new cells by cell proliferation and their degradation by cell death (Abbott et al., 2006; Sweeney et al., 2019).

In vascular endothelial cells, an increase in cytosolic Ca^{2+} concentration ($[Ca^{2+}]_{cyt}$) can influence cell fate, including cell viability and rates of proliferation, migration, and death. Endothelial Ca^{2+} signaling is modulated by the activity of ion channels (Nilius and Droogmans, 2001). BCECs have been reported to express several types of ion channels, such as voltage-dependent K^+ channels, inward-rectifying K^+ (K_{IR}) channels, Ca^{2+}-activated K^+ channels, and transient receptor potential (TRP) channels. Their combined activity contributes to the regulation of brain blood flow (Longden et al., 2016; Sweeney et al., 2019). Previously we have found that small-conductance Ca^{2+}-activated K^+ (SK_{Ca}) channels ($SK_{Ca}2$) (Yamazaki et al., 2006), $K_{IR}2.1$ channels (Yamazaki et al., 2011), TRP canonical subfamily (TRPC) channels (TRPC1/3) (Yamazaki et al., 2007), and store-operated Ca^{2+} channels (Orai1/2 and stromal interaction molecule (STIM) 1) (Kito et al., 2014; Kito et al., 2015) are expressed in BCECs and can facilitate cell proliferation and death. Although the physiological significance of Ca^{2+}

Molecular Pharmacology Fast Forward. Published on May 1, 2020 as DOI: 10.1124/mol.119.118844
This article has not been copyedited and formatted. The final version may differ from this version.

and K^+ channels in BCECs has been examined in detail, that of the functional expression of Cl^- channels remains unclear.

Cl^- channels contribute to a number of physiological processes, such as epithelial fluid secretion, cell volume regulation, osmolarity sensing, smooth muscle contraction, and neuroexcitation. Among Cl^- channels, Ca^{2+}-activated Cl^- (Cl_{Ca}) channels are widely distributed and activated by an increase in $[Ca^{2+}]_{cyt}$. Cl_{Ca} conductance regulates epithelial fluid secretion, smooth muscle contraction, and neurotransmission (Verkman and Galietta, 2009). Two TMEM16 family proteins, TMEM16A and TMEM16B, were recently identified as functional Cl_{Ca} channels. TMEM16A channels are expressed in many cell types, including epithelial cells, smooth muscle cells, the interstitial cells of Cajal (ICC), and nociceptive neurons (Pedemonte and Galietta, 2014). On the other hand, the expression of TMEM16B channels is localized in olfactory, retinal, and hippocampal neurons (Pedemonte and Galietta, 2014). In the TMEM16 research field, the majority of studies focus on physiological and pathological functions in the epithelium, smooth muscles, neurons, and ICC. In contrast, relatively little information has been obtained from the endothelium.

In the present study, the functional expression and physiological significance of the TMEM16 family were examined in mouse BCECs (mBCECs) and a cell line derived from bovine BCECs, t-BBEC117, using Cl_{Ca} channel blockers and TMEM16A small-interfering RNA (siRNA) by quantitative real-time PCR, Western blotting, whole-cell path-clamp, membrane potential and $[Ca^{2+}]_{cyt}$ measurements by fluorescent dyes, cell viability, proliferation, and migration assays, and trans-endothelial permeability measurements. We have found that TMEM16A formed Cl_{Ca} channels in BCECs and strongly modulated both their resting membrane potential and $[Ca^{2+}]_{cyt}$. These changes result in the regulation of the proliferation and migration of these cells.

Materials and Methods

Ethical approval

All experiments were approved by the Ethics Committee of Nagoya City University, and conducted in accordance with the Guide for the Care and Use of Laboratory Animals of the Japanese Pharmacological Society.

Cell isolation

mBCECs were isolated as reported previously (Perrière et al., 2005). In brief, the cerebral cortices of male mice (C57BL/6N, 6~8 weeks; Japan SLC, Hamamatsu, Japan) were removed free of outer blood vessels and meninges and immersed in ice-cold phosphate-buffered saline (PBS). The dissected cortices were homogenized and incubated in Dulbecco's modified Eagle's medium (DMEM, low glucose; Wako Pure Chemical Industries, Osaka, Japan) containing 255 U/ml collagenase (type 2, Worthington Biochemical, Lakewood, NJ), 0.1% dispase II (neutral protease, grade II; Roche Diagnostics, Mannheim, Germany), and 10 U/ml deoxyribonuclease I (from bovine pancreas, type IV; Sigma-Aldrich, St. Louis, MO) at 37°C for 90 min. The digested tissues were centrifuged (1000 rpm, 4°C, 10 min) and the supernatant was removed. The tissue pellet was suspended in DMEM (low glucose) containing 20% bovine serum albumin (fraction V, pH 7.0; Seikagaku, Tokyo, Japan) and centrifuged (1000 rpm, 4°C, 5 min). After the supernatant was removed, the tissue pellet was suspended in DMEM (low glucose) containing 0.1% dispase II and 10 U/ml deoxyribonuclease I, incubated at 37°C for 60 min, and dispersed mechanically. After the supernatant was removed by centrifugation (1000 rpm, 4°C, 5 min), the cell pellet was suspended in DMEM (high glucose; Wako Pure Chemical Industries) containing 15% plasma-derived serum (from platelet poor human plasma; Sigma-Aldrich), 100 U/ml penicillin G (Wako Pure Chemical Industries), 200 μg/ml streptomycin (Meiji Seika Pharma, Tokyo, Japan), and 4 μg/ml puromycin (Invitrogen, Carlsbad, CA), and then filtered

using the Cell Strainers (40 μm; Falcon/Corning, Corning, NY) to obtain the capillary fraction. The capillary cells were incubated on a cell culture dish coated with 0.3 mg/ml collagen (Cellmatrix type IV, Nitta Gelatin, Osaka, Japan) in DMEM (high glucose) supplemented with plasma-derived serum, penicillin G, streptomycin, and puromycin for 48 h. Finally, mBCECs were cultured on a collagen-coated cell culture dish in DMEM (high glucose) supplemented with 15% fetal bovine serum (FBS; Nichirei Biosciences, Tokyo, Japan), penicillin G, and streptomycin.

Cell culture

The immortalized cell line of bovine BCECs, t-BBEC117, was established by transfection of SV40 large T antigen and then by isolating a single clone. *In vitro* culture of these cells has been accompanied by characterization of the BBB phenotypes based on the following criteria: (i) spindle-shape morphology, (ii) rapid uptake of acetylated-low density lipoprotein, (iii) formation of tight junction-like structures, (iv) high alkaline phosphatase activity, and (v) expression of multi-drug resistance and glucose transporter-1 mRNA (Sobue et al., 1999). t-BBEC117 cells were cultured on a non-coating cell culture dish in DMEM (high glucose) supplemented with 10% FBS, 100 U/ml penicillin G, and 10 μg/ml streptomycin. Human embryonic kidney (HEK) 293 cells were obtained from the Japanese Collection of Research Bioresources (JCRB) Cell Bank at the National Institutes of Biomedical Innovation, Health and Nutrition (Osaka, Japan). Normal and TMEM16-expressing HEK293 cells (Saeki et al., 2019) were cultured in DMEM (high glucose) supplemented with 10% FBS, 20 U/ml penicillin G, and 20 μg/ml streptomycin.

Quantitative real-time polymerase chain reaction (PCR)

Total RNA extraction from t-BBEC117 cell homogenates, reverse transcription, and

Molecular Pharmacology Fast Forward. Published on May 1, 2020 as DOI: 10.1124/mol.119.118844
This article has not been copyedited and formatted. The final version may differ from this version.

quantitative real-time PCR using the ABI PRISM 7000 (Applied Biosystems, Foster City, CA) and LightCycler 96 (Roche Diagnostics) real-time PCR systems, were performed as reported previously (Yamazaki et al., 2011). Specific primers for bovine TMEM16 genes were designed as follows: TMEM16A (GenBank Accession number, NM_001192717), (+) CTG GCC TTT GTC ATC GTC TTC, (-) GTG GAT CTG CTG GCT GAT GTC; TMEM16B (XM_024992694), (+) GCC TGG CTG GGA TTA TAT ACA TC, (-) CTC TCT GCT GGG AAT ATC TTC TTC; TMEM16C (NM_001191315), (+) ATT TGC AAG GCC ACT GAA GTC, (-) CAG ATA TGT CAC CTT GGC GTA GA; TMEM16D (NM_001102050), (+) TCC CTC GCT TGG TAT ATG CTT A, (-) TAC AGA CAA GCT GGC ATT CAC A; TMEM16E (NM_001168406), (+) CGT TAT TTG TGG CCT CTT TTC C, (-) CCT GTA CTG AGT CGT AAG CTT CCA; TMEM16F (XM_005206409), (+) CCT GGA CAC CCA CAA GAG TAT AAA, (-) CAC AGA ATA GAT GAC GTG CTC CAT; TMEM16G (XM_024989870), (+) GGT CCA TGG TGC ACT TCA TCT T, (-) AAG GTG GTA ACG AAG CCG AAC T; TMEM16H (XM_024994806), (+) CTG CAG GTA GGT CGG TAT CTG, (-) GTG TGG TCA TCG GTC GTA TCT; TMEM16J (XM_010821300), (+) GGC CCT GGT TCA CTA TGT GAT, (-) GCT CTC TCG CTC TGA AAA GGT; TMEM16K (NM_001102169), (+) CTA TGC CAT CGT GAT CGA GAT, (-) GAT TCT GGT AGG CAG ATT CCA A; and GAPDH (NM_001034034), (+) TTC TGG CAA AGT GGA CAT CGT, (-) CTT GAC TGT GCC GTT GAA CTT G.

Western blot

Western blot experiments were performed as described previously (Yamamura et al., 2018b). In brief, the protein fraction was extracted from mBCECs and t-BBEC117 cell homogenates using RIPA buffer (Cell Signaling Technology, Danvers, MA). The extracted protein (40 µg/lane) was subjected to 7.5% sodium dodecyl sulfate-polyacrylamide gel electrophoresis (SDS-PAGE). After the resulting blots were treated with 5% fat-free milk (Megmilk Snow

Molecular Pharmacology Fast Forward. Published on May 1, 2020 as DOI: 10.1124/mol.119.118844
This article has not been copyedited and formatted. The final version may differ from this version.

Brand, Tokyo, Japan), these were incubated with a polyclonal anti-TMEM16A antibody (1:100; ab53212, Abcam, Cambridge, MA) (Yamamura et al., 2018a) at 4°C for 24 h, treated with an anti-rabbit horseradish peroxidase-conjugated IgG antibody (1:1000; AP132P, Chemicon International, Temecula, CA) at 4°C for 1 h, and then exposed to an enhanced chemiluminescence detection system (Amersham Biosciences, Piscataway, NJ). Protein expression was normalized using monoclonal anti-β-actin (1:2000; A1978, Sigma-Aldrich) and anti-mouse horseradish peroxidase-conjugated IgG (1:5000; AP124P, Chemicon International) antibodies. BCECs, pericytes, and astrocytes were identified by immunoblotting using monoclonal anti-ZO-1 (1:100; sc-33725, Santa Cruz Biotechnology, Dallas, TX), anti-platelet-derived growth factor receptor (PDGFR)-β (1:1000; #3162, Cell Signaling Technology, Danvers, MA), and anti-glia fibrillary acidic protein (GFAP) (1:100; sc-33673, Santa Cruz Biotechnology) antibodies, respectively. The luminescence images were analyzed using a LAS-3000 system (Fujifilm, Tokyo, Japan).

siRNA knockdown

t-BBEC117 cells were cultured to a confluent monolayer (~80%) on a non-coating 60 mm dish. Cultured t-BBEC117 cells were electroporated with 200 nM of control (Medium GC Duplex #3; Invitrogen) or TMEM16A (Stealth RNAi, Tmem16aRSS317801; Invitrogen) siRNA using a Cell Line Nucleofector Kit V (Lonza, Walkersville, MD) by the Nucleofector 2b electroporation system (Lonza). Experiments using siRNA-treated cells were performed 72 h after electroporation.

Electrophysiological recordings

Electrophysiological recordings were performed on single t-BBEC117 cells using a whole-cell patch clamp technique with a CEZ-2400 amplifier (Nihon Kohden, Tokyo, Japan), analog

Molecular Pharmacology Fast Forward. Published on May 1, 2020 as DOI: 10.1124/mol.119.118844
This article has not been copyedited and formatted. The final version may differ from this version.

digital converter (Digidata 1440A; Axon/Molecular Devices, Foster City, CA), and pCLAMP software (version 10; Axon/Molecular Devices), as previously reported (Yamamura et al., 2012). 2-[4-(2-Hydroxyethyl)-1-piperazinyl]ethanesulfonic acid (HEPES)-buffered solution was used as an extracellular solution: 137 mM NaCl, 5.9 mM KCl, 2.2 mM $CaCl_2$, 1.2 mM $MgCl_2$, 14 mM glucose, and 10 mM HEPES. The pH was adjusted to 7.4 with NaOH. The pipette solution had the following ionic composition: 120 mM CsCl, 20 mM tetraethylammonium (TEA)-Cl, 2.8 mM $MgCl_2$, 2 mM $ATPNa_2$, 10 mM HEPES, 5 mM *O,O'*-bis(2-aminoethyl)ethyleneglycol-*N,N,N',N'*-tetraacetic acid (EGTA), and 4.25 mM $CaCl_2$ (pCa 6.0, 1 μM). The pH was adjusted to 7.2 with CsOH. Electrophysiological recordings were performed at room temperature (23~25°C).

Measurement of the membrane potential

Fluorescent changes in the membrane potential were monitored using the ARGUS/HiSCA imaging system (Hamamatsu Photonics, Hamamatsu, Japan). Single t-BBEC117 cells were loaded with the voltage-sensitive fluorescent dye, 100 nM bis(1,3-dibutylbarbituric acid)trimethine oxonol ($DiBAC_4(3)$; Dojin, Kumamoto, Japan), at room temperature for 30 min. $DiBAC_4(3)$ was added to the extracellular solution during measurements. t-BBEC117 cells were illuminated at 488-nm wavelength and the fluorescent emissions (>520 nm) were captured. Fluorescent intensity was normalized by the maximum fluorescence intensity in a 140 mM K^+ solution (F/F_{140K}). Standard HEPES-buffered solution was used as an extracellular solution. The 140 mM K^+ HEPES-buffered solution had the following ionic composition: 5.9 mM NaCl, 140 mM KCl, 2.2 mM $CaCl_2$, 1.2 mM $MgCl_2$, 14 mM glucose, and 10 mM HEPES. The pH was adjusted to 7.4 with NaOH.

$[Ca^{2+}]_{cyt}$ measurements

Molecular Pharmacology Fast Forward. Published on May 1, 2020 as DOI: 10.1124/mol.119.118844
This article has not been copyedited and formatted. The final version may differ from this version.

$[Ca^{2+}]_{cyt}$ measurements were performed using the Argus/HiSCA imaging system. Single t-BBEC117 cells were loaded with 10 μM fura-2 acetoxymethyl ester (fura-2/AM; Molecular Probes/Invitrogen, Eugene, OR) at room temperature for 30 min. The fura-2 signal was converted to $[Ca^{2+}]_{cyt}$ as follows (Yamazaki et al., 2006): $[Ca^{2+}]_{cyt} = K_d \times B \times ((R - R_{min})/(R_{max} - R))$, where K_d is the dissociation constant of fura-2 (224 nM), R is the fluorescence ratio (F_{340}/F_{380}), R_{min} and R_{max} are the fluorescence ratios in the absence of and with the saturation of Ca^{2+}, respectively, and B is the average fluorescence proportionality coefficient obtained at 380 nm under R_{min} and R_{max} conditions ($F^{380}_{min}/F^{380}_{max}$). Standard HEPES-buffered solution was used as an extracellular solution. Ca^{2+}-free HEPES-buffered solution was prepared by adding 1 mM EGTA instead of 2.2 mM $CaCl_2$.

Cell viability assay

t-BBEC117 cells (5×10^3 cells/well) were subcultured in a non-coating 96-well plate and incubated at 37°C for 12 h. Cellular viability was evaluated based on the 3-(4,5-dimethyl-2-thiazolyl)-2,5-diphenyl-2H-tetrazolium bromide (MTT; 5 mg/ml, Sigma-Aldrich) assay, as described previously (Yamazaki et al., 2006). The results obtained were quantified colorimetrically as absorbance at 595 nm using the Multiskan JX (ver.1.1; Thermo Fisher Scientific, Waltham, MA).

Cell proliferation assay

Cell preparation was performed in the same manner as that described for the MTT assay. The proliferation of t-BBEC117 cells was evaluated using the Cell Proliferation ELISA, BrdU (colorimetric) kit (Roche Diagnostics, Mannheim, Germany) based on the bromodeoxyuridine (BrdU) incorporation assay. Colorimetric quantification as absorbance at 450 nm was measured using a similar method to that for the MTT assay.

Molecular Pharmacology Fast Forward. Published on May 1, 2020 as DOI: 10.1124/mol.119.118844
This article has not been copyedited and formatted. The final version may differ from this version.

Wound healing assay

Cell migration was evaluated by a scratch wound assay. t-BBEC117 cells were cultured to a confluent monolayer on a non-coating 24-well plate and then wounded by a sterile 200-μl tip. After the pretreatment with the drug or siRNA for 72 h in DMEM (high glucose) containing 2% FBS, these cells were stained with Hoechst 33342 (1:2000; Molecular Probes/ Invitrogen) at room temperature for 10 min. The number of cells that had migrated into the scratch zone (1 mm × 0.75 mm) for 72 h was counted by the high-content imaging system Operetta (Perkin Elmer Life Sciences, Boston, MA).

Trans-endothelial electrical resistance (TEER) measurements

t-BBEC117 cells (8×10^4 cells/well) were cultured to a confluent monolayer on the Cell Culture Inserts (1.0 μm pore size) and Companion Plates (12-well; Falcon/Corning) for 96 h and then exposed to the drug for 72 h. The TEER of the confluent monolayer of t-BBEC117 cells was measured by the Millicell ERS-2 electrical resistance system (EMD Millipore, Billerica, MA).

Drugs

Pharmacological reagents were obtained from Sigma-Aldrich, except for EGTA and HEPES (Dojin). Niflumic acid (NFA) and $T16A_{inh}$-A01 (2-[(5-ethyl-1,6-dihydro-4-methyl-6-oxo-2-pyrimidinyl)thio]-N-[4-(4-methoxyphenyl)-2-thiazolyl]-acetamide) were dissolved in dimethyl sulfoxide at a concentration of 100 and 10 mM, respectively, as a stock solution.

Statistical analysis

Pooled data are shown as the mean±S.D. The sample size was determined in advance. The significance of differences between two groups was assessed by the Student's *t*-test using the

Molecular Pharmacology Fast Forward. Published on May 1, 2020 as DOI: 10.1124/mol.119.118844
This article has not been copyedited and formatted. The final version may differ from this version.

BellCurve for Excel software (version 3.10; Social Survey Research Information, Tokyo, Japan). The significance of differences among groups was assessed by Tukey's test after a one-way analysis of variance using the same software.

Molecular Pharmacology Fast Forward. Published on May 1, 2020 as DOI: 10.1124/mol.119.118844
This article has not been copyedited and formatted. The final version may differ from this version.

Results

Expression of TMEM16A in BCECs

Expression profile of selected TMEM16 family member in a cell line of bovine BCECs, t-BBEC117, was examined by quantitative real-time PCR and Western blotting. In these t-BBEC117 cells, TMEM16A (0.022±0.007 of GAPDH, n=9) and TMEM16F (0.020±0.015, n=9) were strongly expressed at the mRNA level (Fig. 1A). Since TMEM16A is a confirmed molecular component of Cl_{Ca} channels in various cells (Pedemonte and Galietta, 2014), we have focused on the expression and function of TMEM16A in t-BBEC117 cells. Western blot analysis showed the expression of the TMEM16A protein (114 kDa) in t-BBEC117 cells (n=7; Fig. 1B).

The expression of TMEM16A in native BCECs was examined by Western blotting. BCECs were identified by the presence of ZO-1 protein (BCEC marker) and the absence of PDGFR-β (pericyte marker) and GFAP (astrocyte marker) proteins (n=4; Fig. 1C). TMEM16A was expressed at the protein level in mBCECs (n=4). Collectively, these results strongly suggest that TMEM16A is expressed in BCECs.

Cl_{Ca} currents in t-BBEC117 cells

Whole-cell Cl_{Ca} currents were recorded in t-BBEC117 cells under voltage-clamp conditions. K^+ currents were abolished by Cs^+ and TEA in the pipette solution. Ca^{2+} concentration in the pipette solution was fixed at pCa 6.0 (1 μM). Single cells were depolarized for 500 ms from the holding potential of -40 mV to the selected test potentials (-80~+100 mV) in +20-mV increments, and were then repolarized to -80 mV for 250 ms every 15 s. Cell capacitance averaged 30.9±9.2 pF (n=14). Depolarizations positive to +40 mV evoked time-dependent outward currents (35.9±14.5 pA/pF at +100 mV, n=14; Fig. 2A and B). The time constant for

Molecular Pharmacology Fast Forward. Published on May 1, 2020 as DOI: 10.1124/mol.119.118844
This article has not been copyedited and formatted. The final version may differ from this version.

current activation (τ_{act}) at +100 mV was 244±85 ms (n=14; Fig. 2C). On the other hand, repolarizing stimuli caused characteristic inward tail currents (-33.4±11.3 pA/pF at -80 mV after the +100-mV stimulation, n=14; Fig. 2A). The time constant for tail current deactivation (τ_{tail}) at -80 mV after the +100-mV stimulation was 115±23 ms (n=14; Fig. 2C).

The effects of conventional and selective Cl_{Ca} channel blockers, NFA and $T16A_{inh}$-A01, respectively, on outward and tail currents were examined in t-BBEC117 cells. Both outward and tail currents were strongly inhibited by 100 μM NFA (5.9±1.6 and -7.3±2.9 pA/pF, respectively, n=4, $P<0.05$ versus control; Fig. 2D and E). These currents were also blocked by 10 μM $T16A_{inh}$-A01 (21.1±7.7 and -21.5±7.2 pA/pF, respectively, n=6, $P<0.05$; Fig. 2F and G).

To obtain more direct evidence that the Cl_{Ca} currents in t-BBEC117 cells are mediated by TMEM16A channels, siRNA knockdown experiments on TMEM16A were performed. The knockdown efficiency and selectivity of TMEM16A using a specific siRNA of TMEM16A in t-BBEC117 cells was confirmed by quantitative real-time PCR and Western blotting. The expression of TMEM16A mRNA was reduced markedly by TMEM16A siRNA (by 48%, n=8; Fig. 3A), whereas the mRNA expression of other TMEM16 genes was not changed by TMEM16A siRNA (n=4). However, the possibility of involvement of TMEM16F was unable to be completely removed because the mRNA level was relatively variable in t-BBEC117 cells electroporated with control or TMEM16A siRNA. Expression of the TMEM16A protein was also decreased by TMEM16A siRNA (by 36%, n=4; Fig. 3B). In t-BBEC117 cells electroporated with TMEM16A siRNA, the outward and tail amplitudes of Cl_{Ca} currents were significantly attenuated (14.3±3.9 and -16.0±5.7 pA/pF, n=4, $P<0.05$ versus control siRNA of 32.8±9.7 and -37.7±9.9 pA/pF, n=4, respectively; Fig. 3C and D). Taken together, these results strongly suggest that Cl_{Ca} currents that composed of the TMEM16A-encoding protein and

Molecular Pharmacology Fast Forward. Published on May 1, 2020 as DOI: 10.1124/mol.119.118844
This article has not been copyedited and formatted. The final version may differ from this version.

sensitive to NFA and $T16A_{inh}$-A01 are functionally expressed in t-BBEC117 cells.

Contribution of Cl_{Ca} channels to the resting membrane potential

We next examined whether the activity of Cl_{Ca} channels contributed to the resting membrane potential of t-BBEC117 cells. This was done by monitoring changes in signals from voltage-sensitive fluorescent dye, 100 nM $DiBAC_4(3)$. Membrane potential is presented as F/F_{140K}, where F was the fluorescence intensity and F_{140K} was the maximum fluorescence intensity in the 140 mM K^+ HEPES-buffered solution (theoretically ~0 mV). The fluorescence intensity of $DiBAC_4(3)$ is increased by membrane depolarization and decreased by hyperpolarization. Furthermore, resting membrane potential was hyperpolarized by the application of 100 μM NFA (0.66±0.15, n=45, $P<0.05$ versus control of 0.73±0.12; Fig. 4A and B). Similarly, the resting membrane potential was hyperpolarized by 10 μM $T16A_{inh}$-A01 (0.67±0.15, n=56, $P<0.01$ versus control of 0.81±0.19).

The resting membrane potential was also shifted in the hyperpolarizing direction by the siRNA knockdown of TMEM16A (0.79±0.08, n=66, $P<0.01$ versus control siRNA of 0.84±0.06, n=74; Fig. 4C and D). In t-BBEC117 cells electroporated with TMEM16A siRNA, hyperpolarizing changes in the membrane potential due to the Cl_{Ca} channel blockers, NFA (0.077±0.048, n=22, $P<0.01$ versus control siRNA of 0.139±0.050, n=44) and $T16A_{inh}$-A01 (0.016±0.029, n=44, $P<0.01$ versus control siRNA of 0.092±0.033, n=30), were smaller (Fig. 4C and E). These results indicate that the activity of Cl_{Ca} channels formed by TMEM16A is importantly involved in regulating the resting membrane potential in t-BBEC117 cells.

Effects of TMEM16A siRNA knockdown on resting $[Ca^{2+}]_{cyt}$

Since membrane hyperpolarization often increases $[Ca^{2+}]_{cyt}$ in non-excitable cells, including

Molecular Pharmacology Fast Forward. Published on May 1, 2020 as DOI: 10.1124/mol.119.118844
This article has not been copyedited and formatted. The final version may differ from this version.

BCECs (Guéguinou et al., 2014), the effects of the siRNA knockdown of TMEM16A on resting $[Ca^{2+}]_i$ were examined in t-BBEC117 cells. After t-BBEC117 cells were loaded with the fluorescent Ca^{2+} indicator, 10 μM fura-2/AM, $[Ca^{2+}]_{cyt}$ was measured. TMEM16A siRNA-treated t-BBEC117 cells showed higher $[Ca^{2+}]_{cyt}$ at the resting level (223±77 nM, n=32, P<0.01 versus control siRNA of 144±47 nM, n=40) than control siRNA-electroporated cells (Fig. 5). In combination with the results obtained from membrane potential experiments, reduced TMEM16A channel activity appears to cause membrane hyperpolarization and subsequent $[Ca^{2+}]_{cyt}$ increases in t-BBEC117 cells.

Involvement of Cl_{Ca} channel activity in cell viability and proliferation

Possible contributions of the activity of Cl_{Ca} channels to the viability of t-BBEC117 cells were evaluated using the MTT assay. Cell viability was decreased markedly by the exposure to 100 μM NFA for both 72 h (2.23±0.26, n=16, P<0.05 versus control of 2.90±0.90, n=8) and 96 h (2.76±0.22, n=16, P<0.01 versus control of 4.04±0.65, n=8; Fig. 6A). Similar results were obtained by the application of 30 μM $T16A_{inh}$-A01 for 72 h (2.16±0.17, n=16, P<0.01 versus control of 3.09±1.11, n=8; Fig. 6B). Cell viability was also attenuated concentration-dependently after the 96-h treatment at lower concentrations of 3 μM (2.96±0.36, n=16, P<0.05 versus control of 4.04±0.67, n=8) and 10 μM (3.26±0.59, n=16, P<0.05), as well as 30 μM (2.25±0.30, n=16, P<0.01). In t-BBEC117 cells electroporated with TMEM16A siRNA, cell viability significantly decreased at 72 h (1.58±0.04, n=6, P<0.01 versus control siRNA of 1.76±0.04, n=6) and 96 h (1.67±0.04, n=6, P<0.01 versus control siRNA of 2.04±0.09, n=6; Fig. 6C).

The involvement of Cl_{Ca} channels in the proliferation of t-BBEC117 cells was examined using the BrdU incorporation assay. These results revealed that cell proliferation was reduced by the

Molecular Pharmacology Fast Forward. Published on May 1, 2020 as DOI: 10.1124/mol.119.118844
This article has not been copyedited and formatted. The final version may differ from this version.

treatment with 100 μM NFA (0.15±0.06, n=9, P<0.01 versus control of 0.25±0.05, n=9) or 30 μM T16A$_{inh}$-A01 (0.18±0.05, n=9, P<0.05) for 72 h (Fig. 6D). Furthermore, the siRNA knockdown of TMEM16A also significantly reduced the proliferation of t-BBEC117 cells at 72 h (0.13±0.03, n=6, P<0.05 versus control siRNA of 0.20±0.07, n=6; Fig. 6E). Thus, the activity of TMEM16A Cl_{Ca} channels contributes to regulating of the proliferation of t-BBEC117 cells.

Inhibitory effects of Cl_{Ca} channel blockade on cell migration

To reveal the contributions of Cl_{Ca} channels to cell migration, a wound-healing assay was performed under 2% FBS conditions in t-BBEC117 cells. After the treatment with Cl_{Ca} channel blockers or TMEM16A siRNA, these cells were stained with Hoechst 33342. Then the number of cells that had migrated into the scratch zone was counted by the high-content imaging system Operetta. Migrated cell numbers were significantly decreased by the application of 100 μM NFA (51±3 cells, n=4, P<0.01 versus control of 149±5 cells, n=4; Fig. 7A and B) or 10 μM T16A$_{inh}$-A01 (59±5 cells, n=4, P<0.01) for 72 h. Number of migrated cells were also decreased significantly by TMEM16A siRNA for 72 h (59±12 cells, n=4, P<0.01 versus control siRNA of 167±14 cells, n=4; Fig. 7C and D). In combination, these results strongly suggest that the activity of TMEM16A Cl_{Ca} channels regulates the migration, as well as the proliferation, of t-BBEC117 cells.

Physiological roles of TMEM16A in BBB function

To reveal the involvement of Cl_{Ca} channels in the BBB function, the trans-endothelial permeability of t-BBEC117 cells was analyzed by the TEER measurements. The TEER of the confluent monolayer of t-BBEC117 cells was 24.6±4.7 Ω×cm^2 (n=6; Fig. 8), as reported previously in immortalized cell lines of BCECs (Weksler et al., 2005; Yang et al., 2017). The TEER was significantly decreased by the application of 100 μM NFA (8.1±3.0 Ω×cm^2, n=6,

Molecular Pharmacology Fast Forward. Published on May 1, 2020 as DOI: 10.1124/mol.119.118844
This article has not been copyedited and formatted. The final version may differ from this version.

P<0.01) or 10 μM $T16A_{inh}$-A01 (6.4±1.1 Ω×cm^2, n=6, P<0.01) for 72 h. This result suggests that the activity of TMEM16A Cl_{Ca} channels involves in the regulation of the trans-endothelial permeability in the BBB.

Molecular Pharmacology Fast Forward. Published on May 1, 2020 as DOI: 10.1124/mol.119.118844
This article has not been copyedited and formatted. The final version may differ from this version.

Discussion

In the BBB, BCECs are responsible for its lower permeable barrier function. Accordingly, a delicate balance between the proliferation and death of BCECs is required to maintain BBB functions (Abbott et al., 2006; Sweeney et al., 2019). In various cells, including endothelial cells, cell proliferation and death are modulated by changes in $[Ca^{2+}]_{cyt}$ (Nilius and Droogmans, 2001). Although it is known that changes in $[Ca^{2+}]_{cyt}$ levels in BCECs are modulated strongly by the activity of ion channels, the underlying mechanisms remain unclear. In the present study, we found that a specific type of Cl_{Ca} channels, TMEM16A, are expressed in BCECs. These channels contribute to Cl_{Ca} conductance and participate in determining both the resting membrane potential and $[Ca^{2+}]_{cyt}$, which are involved in the proliferation and migration of BCECs.

In the present study, expression analyses of the TMEM16 family revealed that TMEM16A can be detected at the mRNA and protein levels in mBCECs and t-BBEC117 cells. In addition, in t-BBEC117 cells, relatively large voltage-dependent currents can consistently be recorded under the whole-cell voltage-clamp configuration, after K^+ currents were completely blocked by Cs^+ and TEA, and $[Ca^{2+}]_{cyt}$ was fixed at 1 μM in the pipette solution. Specifically, depolarizing voltage steps to positive membrane potentials elicited a slow time-dependent outward current and subsequent repolarization produced a characteristic inward tail current. The τ_{act} and τ_{deact} of TMEM16A currents ranged between 120~300 and 55~150 ms, respectively (Adomaviciene et al., 2013; Ohshiro et al., 2014b; Scudieri et al., 2013; Yamamura et al., 2018a). In the present study, the kinetic parameters (τ_{act} and τ_{deact}) of Cl_{Ca} currents in t-BBEC117 cells were 244 and 115 ms, respectively, which are similar to those of TMEM16A currents. In addition, these currents were sensitive to a selective blocker of TMEM16A channels, $T16A_{inh}$-A01, as well as to a conventional Cl_{Ca} channel blocker, NFA. The results obtained from the

Molecular Pharmacology Fast Forward. Published on May 1, 2020 as DOI: 10.1124/mol.119.118844
This article has not been copyedited and formatted. The final version may differ from this version.

siRNA knockdown of TMEM16A strongly suggest TMEM16A-encoding Cl_{Ca} currents in t-BBEC117 cells.

Cl_{Ca} channel blockers or TMEM16A siRNA caused membrane hyperpolarization and a subsequent increase in $[Ca^{2+}]_{cyt}$ in BCECs. In non-excitable cells including endothelial cells, membrane hyperpolarization promotes the electrochemical driving force for Ca^{2+} and, thus, facilitates Ca^{2+} influx through voltage-independent Ca^{2+} channels (Guéguinou et al., 2014; Kito et al., 2014; Yamazaki et al., 2011). Cytosolic Cl^- concentration varies widely, 10~60 mM, often in a tissue-dependent manner. Although the cytosolic Cl^- concentration in BCECs is not known, it is estimated to be 30~40 mM in vascular endothelial cells (Kitamura and Yamazaki, 2001). Accordingly, the theoretical equilibrium potential of Cl^- in BCECs may be approximately -30 mV under physiological conditions. The resting membrane potential of t-BBEC117 cells was between -30~-40 mV, as reported previously (Yamamura et al., 2016). Block of Cl_{Ca} channels led to consistent hyperpolarization under our experimental conditions. We previously reported that membrane hyperpolarization following the activation of K^+ channels promoted Ca^{2+} influx through non-selective cation channels in t-BBEC117 cells (Yamazaki et al., 2006; Yamazaki et al., 2011). Similarly, membrane hyperpolarization following Cl_{Ca} channel inhibition also facilitated Ca^{2+} influx through the same signaling pathway as K^+ channel activation.

We previously reported that membrane hyperpolarization and subsequent $[Ca^{2+}]_i$ increases led to BCEC proliferation (Yamazaki et al., 2006), whereas excessive hyperpolarization and abnormal $[Ca^{2+}]_i$ increases induced cell death (Kito et al., 2011; Yamazaki et al., 2011). These effects are mediated by $SK_{Ca}2$ (Yamazaki et al., 2006), $K_{IR}2.1$ (Kito et al., 2011; Yamazaki et al., 2011), TRPC1/3 (Yamazaki et al., 2007), and Orai1/2/STIM1 (Kito et al., 2014; Kito et al., 2015) channels. Furthermore, the present results showed that TMEM16A Cl_{Ca} channels were

Molecular Pharmacology Fast Forward. Published on May 1, 2020 as DOI: 10.1124/mol.119.118844
This article has not been copyedited and formatted. The final version may differ from this version.

involved in regulating the proliferation and migration of BCECs. When Cl_{Ca} channel blockers and the TMEM16A knockdown attenuated the proliferation and migration of BCECs, the IC_{50} value of $T16A_{inh}$-A01 for cell viability was ~10 μM. Since the IC_{50} value for TMEM16A channels was reported to be 1~10 μM in reconstituted and native cells (Davis et al., 2013; Namkung et al., 2011; Ohshiro et al., 2014a; Yamamura et al., 2018a), the inhibitory effects of $T16A_{inh}$-A01 on the proliferation and migration are potentially mediated by TMEM16A Cl_{Ca} channels. Similar inhibitory effects using $T16A_{inh}$-A01 and TMEM16A knockdown were reported in ICC, pancreatic duct cells (Mazzone et al., 2012), and some carcinoma cells, including head and neck squamous (Duvvuri et al., 2012), prostate (Liu et al., 2012), and colorectal (Sui et al., 2014) cancer cells. In contrast, down-regulation of TMEM16A channels can promote the proliferation of rat basilar artery smooth muscle cells (Wang et al., 2012). These quite different effects of TMEM16A channels may be due to differences among cell types. Our results clearly showed that the activity of TMEM16A-encoding Cl_{Ca} channels is a positive regulator of the proliferation and migration of BCECs that maintains the balance between the proliferation and death of these cells in the BBB.

The roles of TMEM16A in cell survival and death, particularly cell proliferation, metastasis, invasiveness, and tumor development in cancer cells, are well established. TMEM16A can activate epidermal growth factor receptor, Ca^{2+}/calmodulin-dependent protein kinase II, mitogen-activated protein kinase, and nuclear factor κB signaling (Wang et al., 2017). However, the signaling mechanisms of TMEM16A for the proliferation and migration of endothelial cells remain unclear. Further studies are needed to elucidate the complete molecular mechanisms associated with TMEM16A for the proliferation and migration of BCECs. In the endothelium, TMEM16A channels were reported to be functionally expressed in cardiac vascular endothelial cells for the prevention of ischemic damage (Wu et al., 2014), umbilical vein endothelial cells

Molecular Pharmacology Fast Forward. Published on May 1, 2020 as DOI: 10.1124/mol.119.118844
This article has not been copyedited and formatted. The final version may differ from this version.

for facilitating reactive oxygen species generation associated in the setting of hypertension (Ma et al., 2017), and brain microvascular endothelial cells for regulating BBB integrity after ischemic stroke (Liu et al., 2019). However, many of physiological and pathological functions of TMEM16A in the endothelium remain unclear. In the present study, we found that the activity of TMEM16A channels partly but substantial contributed to the proliferation and migration of BCECs and the barrier function of the BBB. Since dysfunctions in the BBB can lead to the disruption of homeostasis in the brain, they have been associated with various diseases, such as Alzheimer's disease, Parkinson's disease, amyotrophic lateral sclerosis, multiple sclerosis, stroke, epilepsy, and brain tumors (Abbott et al., 2006; Sweeney et al., 2019). For these reasons, TMEM16A channels may be a novel target for therapeutic drugs for disorders associated with dysfunctions in the BBB.

In conclusion, we have demonstrated that TMEM16A is expressed in BCECs. The activity of TMEM16A Cl_{Ca} channels contributes to regulation of the resting membrane potential and $[Ca^{2+}]_{cyt}$ in BCECs. Both of those signals are crucial for their proliferation and migration. Our results provide novel information on the molecular mechanisms underlying the physiological functions of BCECs in the BBB.

Molecular Pharmacology Fast Forward. Published on May 1, 2020 as DOI: 10.1124/mol.119.118844
This article has not been copyedited and formatted. The final version may differ from this version.

Acknowledgments

We express our sincere thanks to Dr. Wayne R. Giles (University of Calgary, Calgary, Canada) for critical reading and editing of this manuscript. We also thank Dr. Tamihide Matsunaga and Ms. Misaki Yamashita (Nagoya City University, Nagoya, Japan) for technical supports. We acknowledge the assistance of the Research Equipment Sharing Center at the Nagoya City University.

Authorship contributions

Participated in research design: T. Suzuki, Imaizumi, and Yamamura.

Conducted experiments: T. Suzuki, Yasumoto.

Contributed new reagents or analytic tools: Asai.

Performed data analysis: T. Suzuki, Yasumoto, Y. Suzuki, Imaizumi, and Yamamura.

Wrote or contributed to the writing of the manuscript: T. Suzuki and Yamamura.

References

Abbott NJ, Rönnbäck L and Hansson E (2006) Astrocyte-endothelial interactions at the blood-brain barrier. *Nat Rev Neurosci* **7**(1): 41-53.

Adomaviciene A, Smith KJ, Garnett H and Tammaro P (2013) Putative pore-loops of TMEM16/anoctamin channels affect channel density in cell membranes. *J Physiol* **591**(14): 3487-3505.

Davis AJ, Shi J, Pritchard HA, Chadha PS, Leblanc N, Vasilikostas G, Yao Z, Verkman AS, Albert AP and Greenwood IA (2013) Potent vasorelaxant activity of the TMEM16A inhibitor $T16A_{inh}$-A01. *Br J Pharmacol* **168**(3): 773-784.

Duvvuri U, Shiwarski DJ, Xiao D, Bertrand C, Huang X, Edinger RS, Rock JR, Harfe BD, Henson BJ, Kunzelmann K, Schreiber R, Seethala RS, Egloff AM, Chen X, Lui VW, Grandis JR and Gollin SM (2012) TMEM16A induces MAPK and contributes directly to tumorigenesis and cancer progression. *Cancer Res* **72**(13): 3270-3281.

Guéguinou M, Chantôme A, Fromont G, Bougnoux P, Vandier C and Potier-Cartereau M (2014) KCa and Ca^{2+} channels: the complex thought. *Biochim Biophys Acta* **1843**(10): 2322-2333.

Kitamura K and Yamazaki J (2001) Chloride channels and their functional roles in smooth muscle tone in the vasculature. *Jpn J Pharmacol* **85**(4): 351-357.

Kito H, Yamamura H, Suzuki Y, Ohya S, Asai K and Imaizumi Y (2014) Membrane hyperpolarization induced by endoplasmic reticulum stress facilitates Ca^{2+} influx to regulate cell cycle progression in brain capillary endothelial cells. *J Pharmacol Sci* **125**(2): 227-232.

Kito H, Yamamura H, Suzuki Y, Yamamura H, Ohya S, Asai K and Imaizumi Y (2015) Regulation of store-operated Ca^{2+} entry activity by cell cycle dependent up-regulation of Orai2 in brain capillary endothelial cells. *Biochem Biophys Res Commun* **459**(3): 457-

462.

Kito H, Yamazaki D, Ohya S, Yamamura H, Asai K and Imaizumi Y (2011) Up-regulation of $K_{ir}2.1$ by ER stress facilitates cell death of brain capillary endothelial cells. *Biochem Biophys Res Commun* **411**(2): 293-298.

Liu PY, Zhang Z, Liu Y, Tang XL, Shu S, Bao XY, Zhang Y, Gu Y, Xu Y and Cao X (2019) TMEM16A inhibition preserves blood-brain barrier integrity after ischemic stroke. *Front Cell Neurosci* **13**: 360.

Liu W, Lu M, Liu B, Huang Y and Wang K (2012) Inhibition of Ca^{2+}-activated Cl^- channel ANO1/TMEM16A expression suppresses tumor growth and invasiveness in human prostate carcinoma. *Cancer Lett* **326**(1): 41-51.

Longden TA, Hill-Eubanks DC and Nelson MT (2016) Ion channel networks in the control of cerebral blood flow. *J Cereb Blood Flow Metab* **36**(3): 492-512.

Ma MM, Gao M, Guo KM, Wang M, Li XY, Zeng XL, Sun L, Lv XF, Du YH, Wang GL, Zhou JG and Guan YY (2017) TMEM16A contributes to endothelial dysfunction by facilitating Nox2 NADPH oxidase-derived reactive oxygen species generation in hypertension. *Hypertension* **69**(5): 892-901.

Mazzone A, Eisenman ST, Strege PR, Yao Z, Ordog T, Gibbons SJ and Farrugia G (2012) Inhibition of cell proliferation by a selective inhibitor of the Ca^{2+}-activated Cl^- channel, Ano1. *Biochem Biophys Res Commun* **427**(2): 248-253.

Nakagawa S, Deli MA, Kawaguchi H, Shimizudani T, Shimono T, Kittel A, Tanaka K and Niwa M (2009) A new blood-brain barrier model using primary rat brain endothelial cells, pericytes and astrocytes. *Neurochem Int* **54**(3-4): 253-263.

Namkung W, Phuan PW and Verkman AS (2011) TMEM16A inhibitors reveal TMEM16A as a minor component of calcium-activated chloride channel conductance in airway and intestinal epithelial cells. *J Biol Chem* **286**(3): 2365-2374.

Nilius B and Droogmans G (2001) Ion channels and their functional role in vascular endothelium. *Physiol Rev* **81**(4): 1415-1459.

Ohshiro J, Yamamura H, Saeki T, Suzuki Y and Imaizumi Y (2014a) The multiple expression of Ca^{2+}-activated Cl^- channels via homo- and hetero-dimer formation of TMEM16A splicing variants in murine portal vein. *Biochem Biophys Res Commun* **443**(2): 518-523.

Ohshiro J, Yamamura H, Suzuki Y and Imaizumi Y (2014b) Modulation of TMEM16A-channel activity as Ca^{2+} activated Cl^- conductance via the interaction with actin cytoskeleton in murine portal vein. *J Pharmacol Sci* **125**(1): 107-111.

Pedemonte N and Galietta LJ (2014) Structure and function of TMEM16 proteins (anoctamins). *Physiol Rev* **94**(2): 419-459.

Perrière N, Demeuse P, Garcia E, Regina A, Debray M, Andreux JP, Couvreur P, Scherrmann JM, Temsamani J, Couraud PO, Deli MA and Roux F (2005) Puromycin-based purification of rat brain capillary endothelial cell cultures. Effect on the expression of blood-brain barrier-specific properties. *J Neurochem* **93**(2): 279-289.

Saeki T, Kimura T, Hashidume K, Murayama T, Yamamura H, Ohya S, Suzuki Y, Nakayama S and Imaizumi Y (2019) Conversion of Ca^{2+} oscillation into propagative electrical signals by Ca^{2+}-activated ion channels and connexin as a reconstituted Ca^{2+} clock model for the pacemaker activity. *Biochem Biophys Res Commun* **510**(2): 242-247.

Scudieri P, Sondo E, Caci E, Ravazzolo R and Galietta LJ (2013) TMEM16A-TMEM16B chimaeras to investigate the structure-function relationship of calcium-activated chloride channels. *Biochem J* **452**(3): 443-455.

Sobue K, Yamamoto N, Yoneda K, Hodgson ME, Yamashiro K, Tsuruoka N, Tsuda T, Katsuya H, Miura Y, Asai K and Kato T (1999) Induction of blood-brain barrier properties in immortalized bovine brain endothelial cells by astrocytic factors. *Neurosci Res* **35**(2): 155-164.

Sui Y, Sun M, Wu F, Yang L, Di W, Zhang G, Zhong L, Ma Z, Zheng J, Fang X and Ma T (2014) Inhibition of TMEM16A expression suppresses growth and invasion in human colorectal cancer cells. *PLoS One* **9**(12): e115443.

Sweeney MD, Zhao Z, Montagne A, Nelson AR and Zlokovic BV (2019) Blood-brain barrier: From physiology to disease and back. *Physiol Rev* **99**(1): 21-78.

Verkman AS and Galietta LJ (2009) Chloride channels as drug targets. *Nat Rev Drug Discov* **8**(2): 153-171.

Wang H, Zou L, Ma K, Yu J, Wu H, Wei M and Xiao Q (2017) Cell-specific mechanisms of TMEM16A Ca^{2+}-activated chloride channel in cancer. *Mol Cancer* **16**(1): 152.

Wang M, Yang H, Zheng LY, Zhang Z, Tang YB, Wang GL, Du YH, Lv XF, Liu J, Zhou JG and Guan YY (2012) Downregulation of TMEM16A calcium-activated chloride channel contributes to cerebrovascular remodeling during hypertension by promoting basilar smooth muscle cell proliferation. *Circulation* **125**(5): 697-707.

Weksler BB, Subileau EA, Perrière N, Charneau P, Holloway K, Leveque M, Tricoire-Leignel H, Nicotra A, Bourdoulous S, Turowski P, Male DK, Roux F, Greenwood J, Romero IA and Couraud PO (2005) Blood-brain barrier-specific properties of a human adult brain endothelial cell line. *FASEB J* **19**(13): 1872-1874.

Wu MM, Lou J, Song BL, Gong YF, Li YC, Yu CJ, Wang QS, Ma TX, Ma K, Hartzell HC, Duan DD, Zhao D and Zhang ZR (2014) Hypoxia augments the calcium-activated chloride current carried by anoctamin-1 in cardiac vascular endothelial cells of neonatal mice. *Br J Pharmacol* **171**(15): 3680-3692.

Yamamura H, Ikeda C, Suzuki Y, Ohya S and Imaizumi Y (2012) Molecular assembly and dynamics of fluorescent protein-tagged single $K_{Ca}1.1$ channel in expression system and vascular smooth muscle cells. *Am J Physiol Cell Physiol* **302**(8): C1257-1268.

Yamamura H, Nishimura K, Hagihara Y, Suzuki Y and Imaizumi Y (2018a) TMEM16A and

TMEM16B channel proteins generate Ca^{2+}-activated Cl^- current and regulate melatonin secretion in rat pineal glands. *J Biol Chem* **293**(3): 995-1006.

Yamamura H, Suzuki Y, Yamamura H, Asai K, Giles W and Imaizumi Y (2018b) Hypoxic stress upregulates $K_{ir}2.1$ expression by a pathway including hypoxic-inducible factor-1α and dynamin2 in brain capillary endothelial cells. *Am J Physiol Cell Physiol* **315**(2): C202-C213.

Yamamura H, Suzuki Y, Yamamura H, Asai K and Imaizumi Y (2016) Hypoxic stress up-regulates Kir2.1 expression and facilitates cell proliferation in brain capillary endothelial cells. *Biochem Biophys Res Commun* **476**(4): 386-392.

Yamazaki D, Aoyama M, Ohya S, Muraki K, Asai K and Imaizumi Y (2006) Novel functions of small conductance Ca^{2+}-activated K^+ channel in enhanced cell proliferation by ATP in brain endothelial cells. *J Biol Chem* **281**(50): 38430-38439.

Yamazaki D, Kito H, Yamamoto S, Ohya S, Yamamura H, Asai K and Imaizumi Y (2011) Contribution of $K_{ir}2$ potassium channels to ATP-induced cell death in brain capillary endothelial cells and reconstructed HEK293 cell model. *Am J Physiol Cell Physiol* **300**(1): C75-86.

Yamazaki D, Ohya S, Asai K and Imaizumi Y (2007) Characteristics of the ATP-induced Ca^{2+}-entry pathway in the t-BBEC 117 cell line derived from bovine brain endothelial cells. *J Pharmacol Sci* **104**(1): 103-107.

Yang S, Mei S, Jin H, Zhu B, Tian Y, Huo J, Cui X, Guo A and Zhao Z (2017) Identification of two immortalized cell lines, ECV304 and bEnd3, for *in vitro* permeability studies of blood-brain barrier. *PLoS One* **12**(10): e0187017.

Molecular Pharmacology Fast Forward. Published on May 1, 2020 as DOI: 10.1124/mol.119.118844
This article has not been copyedited and formatted. The final version may differ from this version.

Footnotes

This work was supported by a Grant-in-Aid for Scientific Research on Innovative Areas (17H05537 to H. Yamamura), Grants-in-Aid for Promotion of Joint International Research (Fostering Joint International Research (B)) (18KK0218 to Y. Imaizumi), Grants-in-Aid for Scientific Research (B) (19H03381 to Y. Suzuki), and Grants-in Aid for Scientific Research (C) (16K08278 and 19K07125 to H. Yamamura) from the Japan Society for the Promotion of Science. This work was partly supported by a Grant-in-Aid for the Suzuken Memorial Foundation. T. Suzuki holds a Ph.D. scholarship from the Kidani Memorial Trust.

Reprint requests

Dr. Hisao Yamamura, Department of Molecular and Cellular Pharmacology, Graduate School of Pharmaceutical Sciences, Nagoya City University, 3-1 Tanabedori, Mizuhoku, Nagoya 467-8603, Japan. E-mail: yamamura@phar.nagoya-cu.ac.jp

Molecular Pharmacology Fast Forward. Published on May 1, 2020 as DOI: 10.1124/mol.119.118844
This article has not been copyedited and formatted. The final version may differ from this version.

Figure legends

Fig. 1. Expression analyses of the TMEM16 family in BCECs

Expression profile of TMEM16 genes (TMEM16A to K except for I) in a cell line of bovine BCECs, t-BBEC117, and mBCECs was examined by quantitative real-time PCR and Western blotting. **A:** Quantitative real-time PCR analysis of TMEM16 candidates. Note that mRNA expression of TMEM16A and TMEM16F is abundant in t-BBEC117 cells (n=9). The Ct value of GAPDH was 17.4±1.2 (n=9). **B:** Western blot analysis of TMEM16A (114 kDa) and β-actin (42 kDa) in t-BBEC117 cells. Normal and TMEM16A-expressing HEK293 cells were used as positive and negative controls for TMEM16A expression. Similar results were obtained from 7 independent experiments. **C:** Western blot analysis of TMEM16A with ZO-1 (BCEC marker), PDGFR-β (pericyte marker), GFAP (astrocyte marker), and β-actin in mBCECs (n=4). Data are shown as mean±S.D.

Fig. 2. Whole-cell Cl_{Ca} currents in t-BBEC117 cells

Cl_{Ca} currents were recorded in t-BBEC117 cells under the whole-cell voltage-clamp configuration. K^+ currents were abolished by Cs^+ and TEA, and $[Ca^{2+}]_{cyt}$ was fixed at pCa 6.0 (1 μM) in the pipette solution. Single cells were depolarized for 500 ms from the holding potential of -40 mV to test potentials (-80~+100 mV) in +20-mV increments and subsequently repolarized for 250 ms to -80 mV every 15 s. **A:** A representative trace of whole-cell Cl_{Ca} currents in t-BBEC117 cells. Note that time-dependent outward currents and inward tail currents, which are characteristic of Cl_{Ca} currents, were observed. **B:** Current density-voltage relationship (n=14). **C:** τ_{act} and τ_{tail} of Cl_{Ca} currents (n=14). **D:** Representative traces of Cl_{Ca} currents in the absence and presence of 100 μM NFA. **E:** Inhibitory effects of NFA on outward (at +100 mV; peak) and inward (at -80 mV following +100 mV depolarization; tail) current densities (n=4). **F:** Representative Cl_{Ca} currents in the absence and presence of 10 μM $T16A_{inh}$-

Molecular Pharmacology Fast Forward. Published on May 1, 2020 as DOI: 10.1124/mol.119.118844
This article has not been copyedited and formatted. The final version may differ from this version.

A01 (T16A). **G:** Inhibitory effects of $T16A_{inh}$-A01 on outward and inward current densities (n=6). Data are shown as mean±S.D. *P<0.05, **P<0.01 versus control (paired t-test).

Fig. 3. Reduced Cl_{Ca} currents by the TMEM16A knockdown

Effects of siRNA knockdown of TMEM16A on Cl_{Ca} currents in t-BBEC117 cells were examined. **A:** Knockdown efficiency and selectivity of TMEM16A siRNA were confirmed in t-BBEC117 cells using quantitative real-time PCR method (n=4~8). The Ct value of GAPDH was 17.0±1.3 (n=8). **B:** Knockdown efficiency of TMEM16A siRNA was confirmed in t-BBEC117 cells by Western blotting. Similar results were obtained from 4 independent experiments. **C:** Representative Cl_{Ca} current records from t-BBEC117 cells that had been electroporated with either control (siControl) or TMEM16A (siTMEM16A) siRNA. These single cells were depolarized for 500 ms from the holding potential of -40 mV to test potentials (-80~+100 mV) by +20-mV increments and subsequently repolarized to -80 mV for 250 ms every 15 s. **D:** Summarized data of outward (at +100 mV; peak) and inward (at -80 mV following +100-mV depolarization; tail) current densities in t-BBEC117 cells electroporated with control or TMEM16A siRNA (n=4). Data are shown as mean±S.D. *P<0.05, **P<0.01 versus control siRNA (unpaired two-tailed t-test).

Fig. 4. Contribution of Cl_{Ca} channels to the resting membrane potential

Effects of selected Cl_{Ca} channel blockers on the resting membrane potential were monitored in t-BBEC117 cells that had been loaded with the voltage-sensitive fluorescent indicator, 100 nM $DiBAC_4(3)$. Fluorescent intensity of $DiBAC_4(3)$ was increased and decreased by membrane depolarization and hyperpolarization, respectively. Fluorescent intensity signal was normalized by the maximum fluorescent intensity in the 140 mM K^+ HEPES-buffered solution (F/F_{140K}). **A:** Representative time-courses of the membrane potential in t-BBEC117 cells. Note that block

Molecular Pharmacology Fast Forward. Published on May 1, 2020 as DOI: 10.1124/mol.119.118844
This article has not been copyedited and formatted. The final version may differ from this version.

of Cl_{Ca} channels by 100 μM NFA and 10 μM $T16A_{inh}$-A01 (T16A) caused membrane hyperpolarization. **B:** Effects of NFA (n=45) and $T16A_{inh}$-A01 (n=56) on the resting membrane potential. **C:** Representative time courses of the membrane potential in the absence and presence of Cl_{Ca} channel blockers in t-BBEC117 cells that had been electroporated with control (siControl) or TMEM16A (siTMEM16A) siRNA. **D:** Summarized data of the resting membrane potential in control (n=74) or TMEM16A (n=66) siRNA-electroporated t-BBEC117 cells. **E:** Sensitivities to Cl_{Ca} channel blockers on the resting membrane potential in t-BBEC117 cells that had been electroporated with control or TMEM16A siRNA (n=22~44). Data are shown as mean±S.D. *P<0.05, **P<0.01 versus control or control siRNA (paired t-test for B; unpaired two-tailed t-test for D, E).

Fig. 5. Effects of the TMEM16A siRNA knockdown on resting $[Ca^{2+}]_{cyt}$

The effects of the siRNA knockdown of TMEM16A on resting $[Ca^{2+}]_{cyt}$ measured in t-BBEC117 cells loaded with the Ca^{2+}-sensitive fluorescent indicator, fura-2/AM. **A:** $[Ca^{2+}]_{cyt}$ levels in t-BBEC117 cells that had been electroporated with control (siControl; n=40) or TMEM16A (siTMEM16A; n=32) siRNA. **B:** Summarized data of $[Ca^{2+}]_{cyt}$ in control (n=40) or TMEM16A (n=32) siRNA-electroporated t-BBEC117 cells. Data are shown as mean±S.D. **P<0.01 versus control siRNA (unpaired two-tailed t-test).

Fig. 6. Involvement of TMEM16A Cl_{Ca} channel activity on cell viability and proliferation

The involvement of the activity of Cl_{Ca} channels mediated by TMEM16A expression on the viability and proliferation of t-BBEC117 cells was examined by the MTT and BrdU assays, respectively. **A:** Effects of a conventional Cl_{Ca} channel blocker, 100 μM NFA, on the viability of t-BBEC117 cells (n=8~16). Data were normalized at 0 h (1.0). **B:** Effects of a selective Cl_{Ca} channel blocker, $T16A_{inh}$-A01 (T16A) on cell viability (n=8~16). Note that the inhibitory effect

Molecular Pharmacology Fast Forward. Published on May 1, 2020 as DOI: 10.1124/mol.119.118844
This article has not been copyedited and formatted. The final version may differ from this version.

on cell viability was concentration-dependent. **C:** Inhibitory effects of TMEM16A siRNA on cell viability (n=6). **D:** Effects of Cl_{Ca} channel blockers on the proliferation of t-BBEC117 cells (n=9). **E:** Reduced cell proliferation by the treatment with TMEM16A siRNA (n=6). Data are shown as mean±S.D. *P<0.05, **P<0.01 versus control or control siRNA (unpaired two-tailed t-test for A, C, E; Tukey's test for B, D).

Fig. 7. Contribution of TMEM16A Cl_{Ca} channels to cell migration

To examine the contributions of TMEM16A Cl_{Ca} channels on the migration of t-BBEC117 cells, a wound-healing assay was performed in DMEM (high glucose) containing 2% FBS. After the treatment with Cl_{Ca} channel blockers or TMEM16A siRNA, these cells were stained with Hoechst 33342. The number of cells that had migrated into the scratch zone was counted by the high-content imaging system Operetta. Dotted lines indicate the 'scratch zone' at 0 h, the start of this experiment. **A:** Representative images showing the migration of t-BBEC117 cells before (0 h) and after (72 h) the treatment with the Cl_{Ca} channel blockers, 100 μM NFA and 10 μM $T16A_{inh}$-A01 (T16A). **B:** Summarized data showing inhibitory effects of the Cl_{Ca} channel blockers, NFA and $T16A_{inh}$-A01, on cell migration (n=4). **C:** Representative images of the migration of t-BBEC117 cells before (0 h) and after (72 h) treatment with TMEM16A siRNA. **D:** Summarized data showing the migration of t-BBEC117 cells electroporated with control (siControl) or TMEM16A (siTMEM16A) siRNA (n=4). Data are shown as mean±S.D. **P<0.01 versus control or control siRNA (Tukey's test for A; unpaired two-tailed t-test for D).

Fig. 8. Effects of Cl_{Ca} channel blockers on trans-endothelial permeability

To reveal the involvement of Cl_{Ca} channels in the trans-endothelial permeability, the TEER of the confluent monolayer of t-BBEC117 cells was measured. Summarized data showing effects of the Cl_{Ca} channel blockers, NFA and $T16A_{inh}$-A01 (T16A), on the TEER (n=6). Data are

Molecular Pharmacology Fast Forward. Published on May 1, 2020 as DOI: 10.1124/mol.119.118844
This article has not been copyedited and formatted. The final version may differ from this version.

shown as mean±S.D. **P<0.01 versus control (Tukey's test).

Figure 1

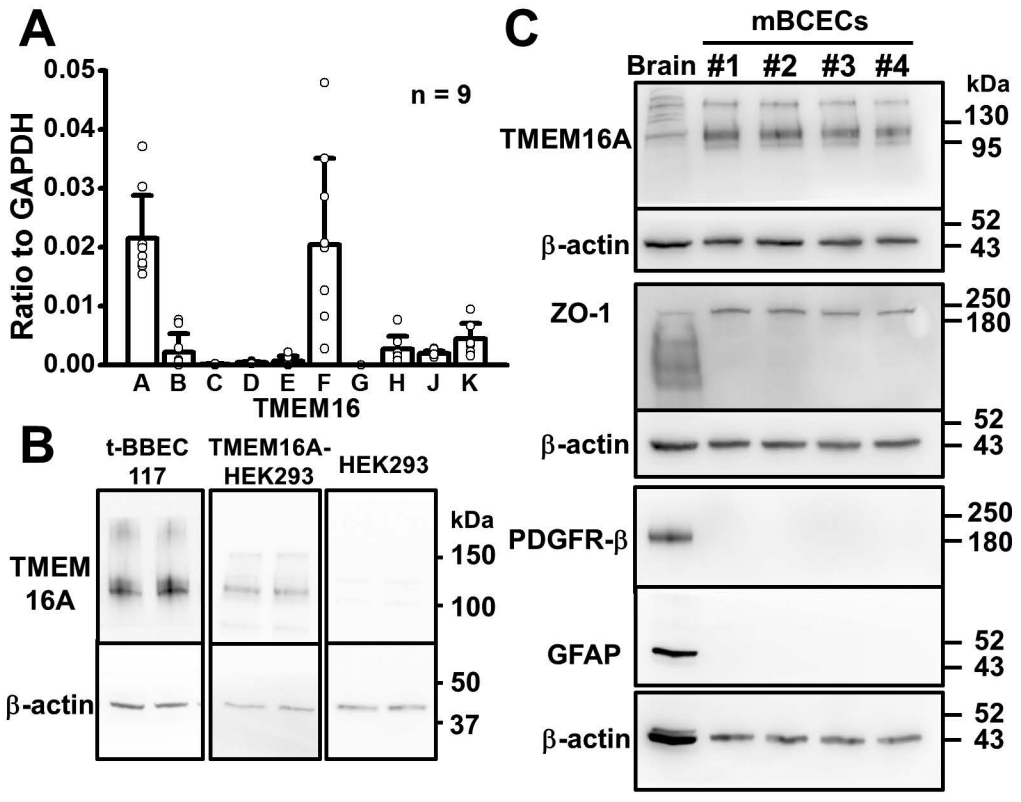
A
Ratio to GAPDH
0.05
0.04
0.03
0.02
0.01
0.00
n = 9
A B C D E F G H J K
TMEM16
B
t-BBEC 117
TMEM16A-HEK293
HEK293
TMEM 16A
β-actin
kDa
150
100
50
37
C
mBCECs
Brain #1 #2 #3 #4
TMEM16A
β-actin
ZO-1
β-actin
PDGFR-β
GFAP
β-actin
kDa
130
95
52
43
250
180
52
43
250
180
52
43
52
43

Figure 2

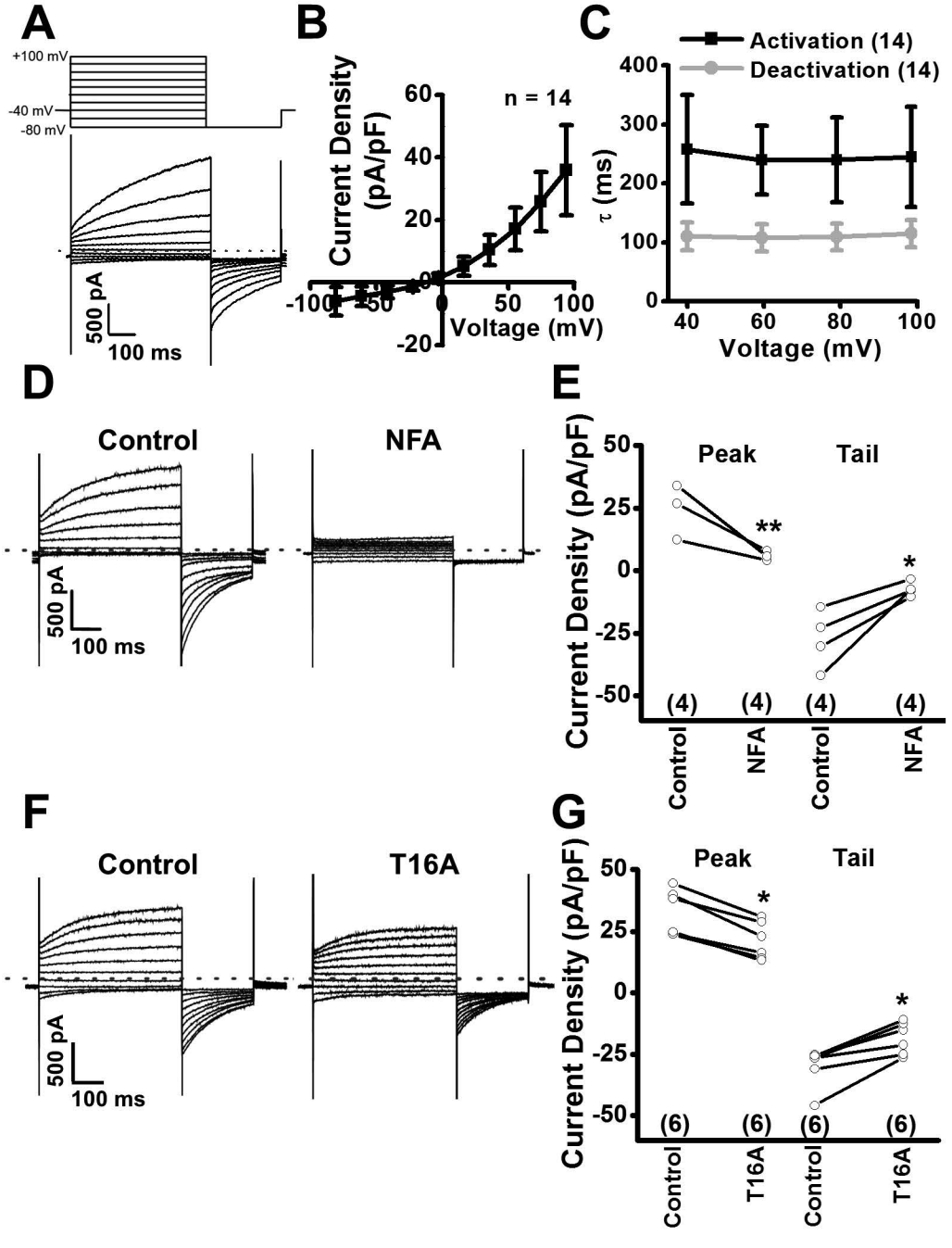
A
+100 mV
-40 mV
-80 mV
500 pA
100 ms
B
Current Density (pA/pF)
n = 14
Voltage (mV)
C
Activation (14)
Deactivation (14)
τ (ms)
Voltage (mV)
D
Control
NFA
500 pA
100 ms
E
Current Density (pA/pF)
Peak
Tail
(4)
Control
NFA
F
Control
T16A
500 pA
100 ms
G
Current Density (pA/pF)
Peak
Tail
(6)
Control
T16A

Figure 3

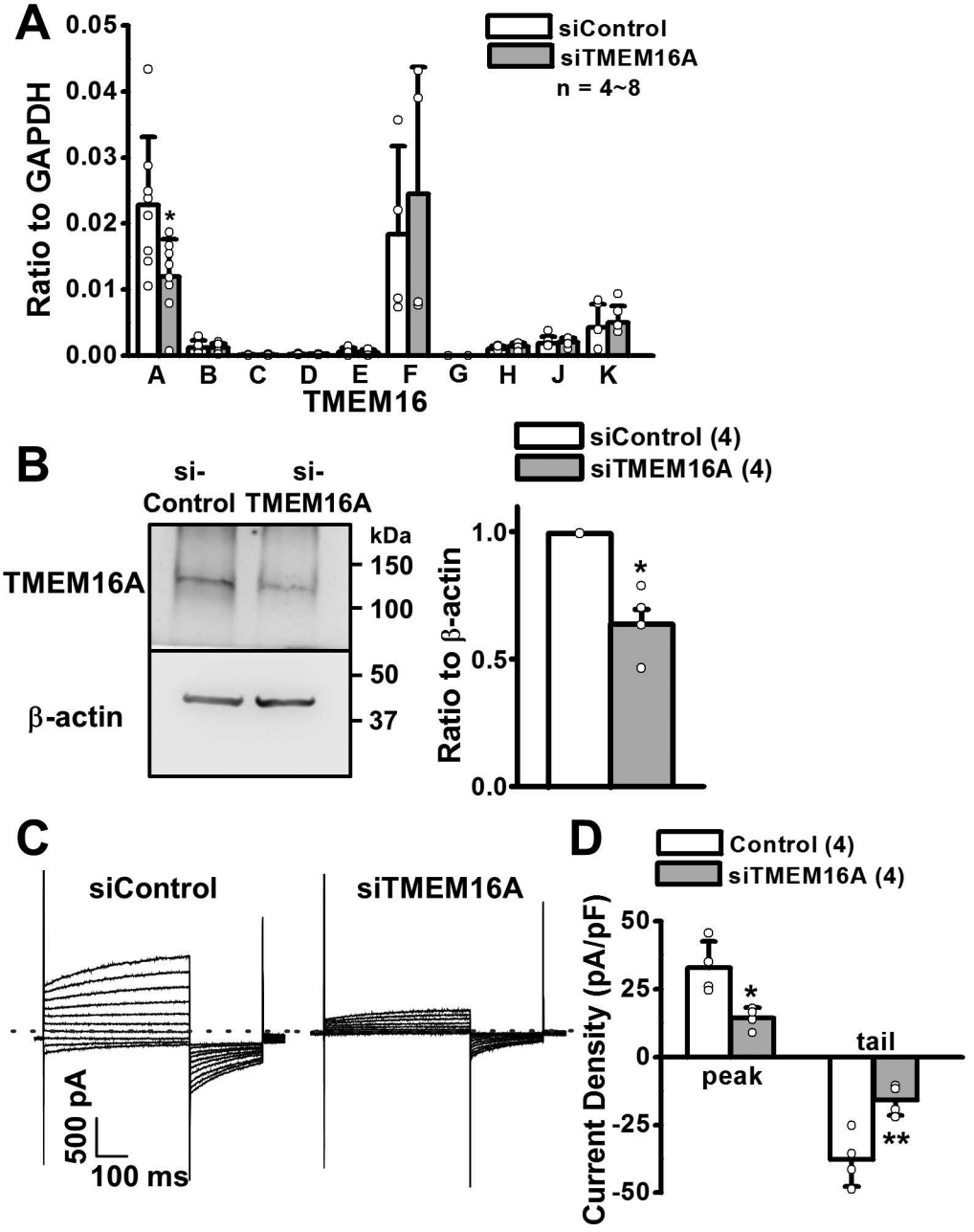
A
siControl
siTMEM16A
n = 4~8
Ratio to GAPDH
0.05
0.04
0.03
0.02
0.01
0.00
*
A B C D E F G H J K
TMEM16
B
si-Control
si-TMEM16A
kDa
TMEM16A
150
100
β-actin
50
37
siControl (4)
siTMEM16A (4)
Ratio to β-actin
1.0
0.5
0.0
*
C
siControl
siTMEM16A
500 pA
100 ms
D
Control (4)
siTMEM16A (4)
Current Density (pA/pF)
50
25
0
-25
-50
*
peak
tail
**

Figure 4

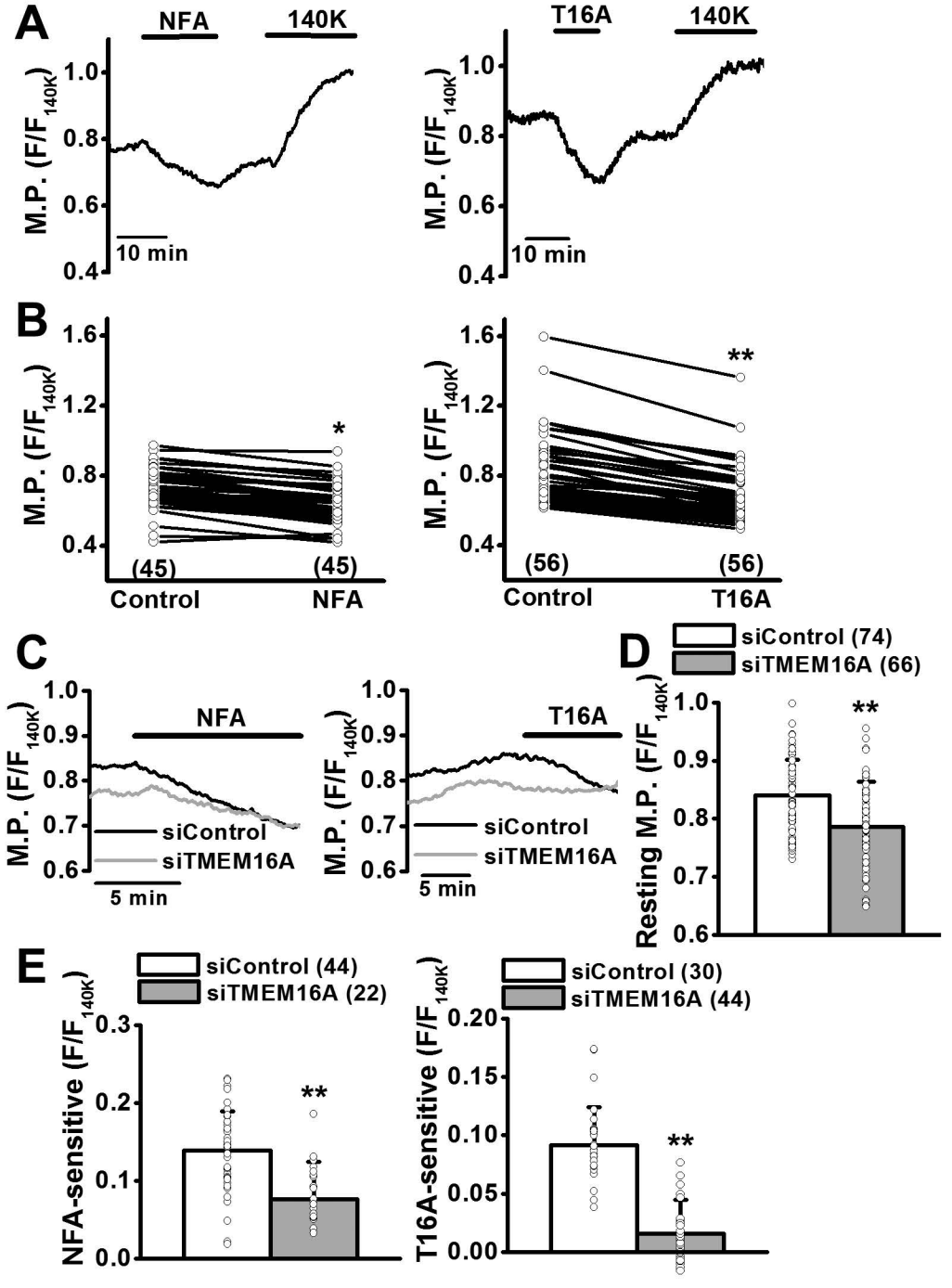
A
NFA
140K
T16A
140K
M.P. (F/F140K)
1.0
0.8
0.6
0.4
10 min
B
1.6
1.2
0.8
0.4
*
**
(45)
(45)
(56)
(56)
Control
NFA
Control
T16A
C
NFA
T16A
siControl
siTMEM16A
5 min
D
siControl (74)
siTMEM16A (66)
Resting M.P. (F/F140K)
E
siControl (44)
siTMEM16A (22)
NFA-sensitive (F/F140K)
0.3
0.2
0.1
0.0
siControl (30)
siTMEM16A (44)
T16A-sensitive (F/F140K)
0.20
0.15
0.10
0.05
0.00

Figure 5

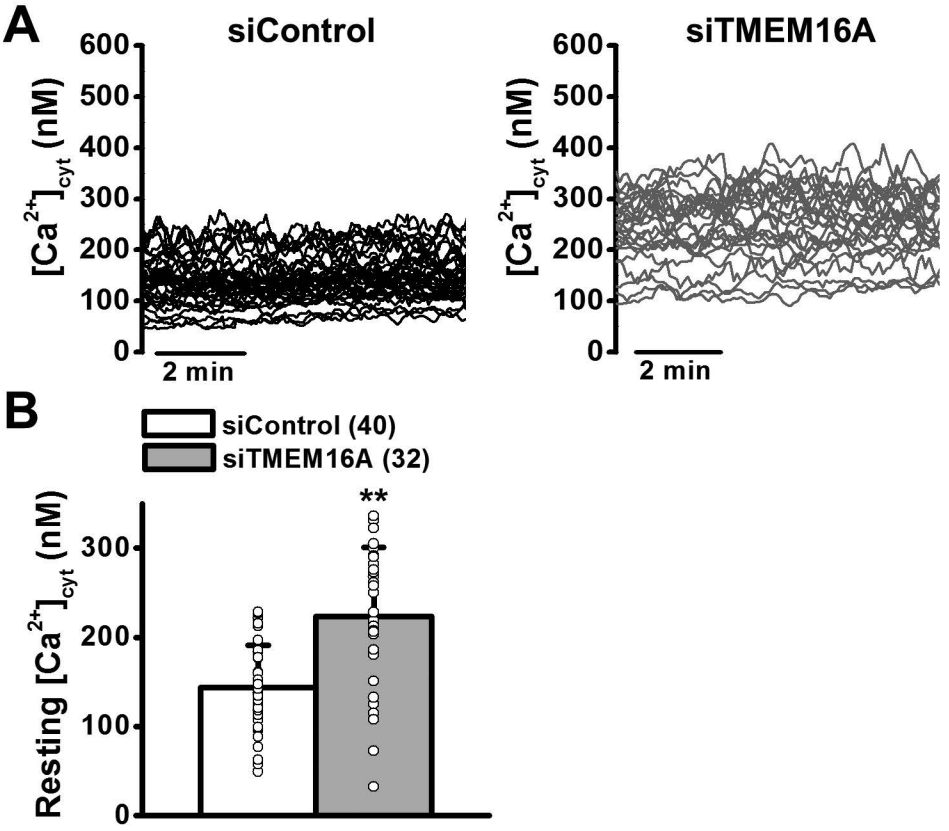
A
siControl
siTMEM16A
600
500
400
300
200
100
0
[Ca2+]cyt (nM)
2 min
B
siControl (40)
siTMEM16A (32)
Resting [Ca2+]cyt (nM)
**

Figure 6

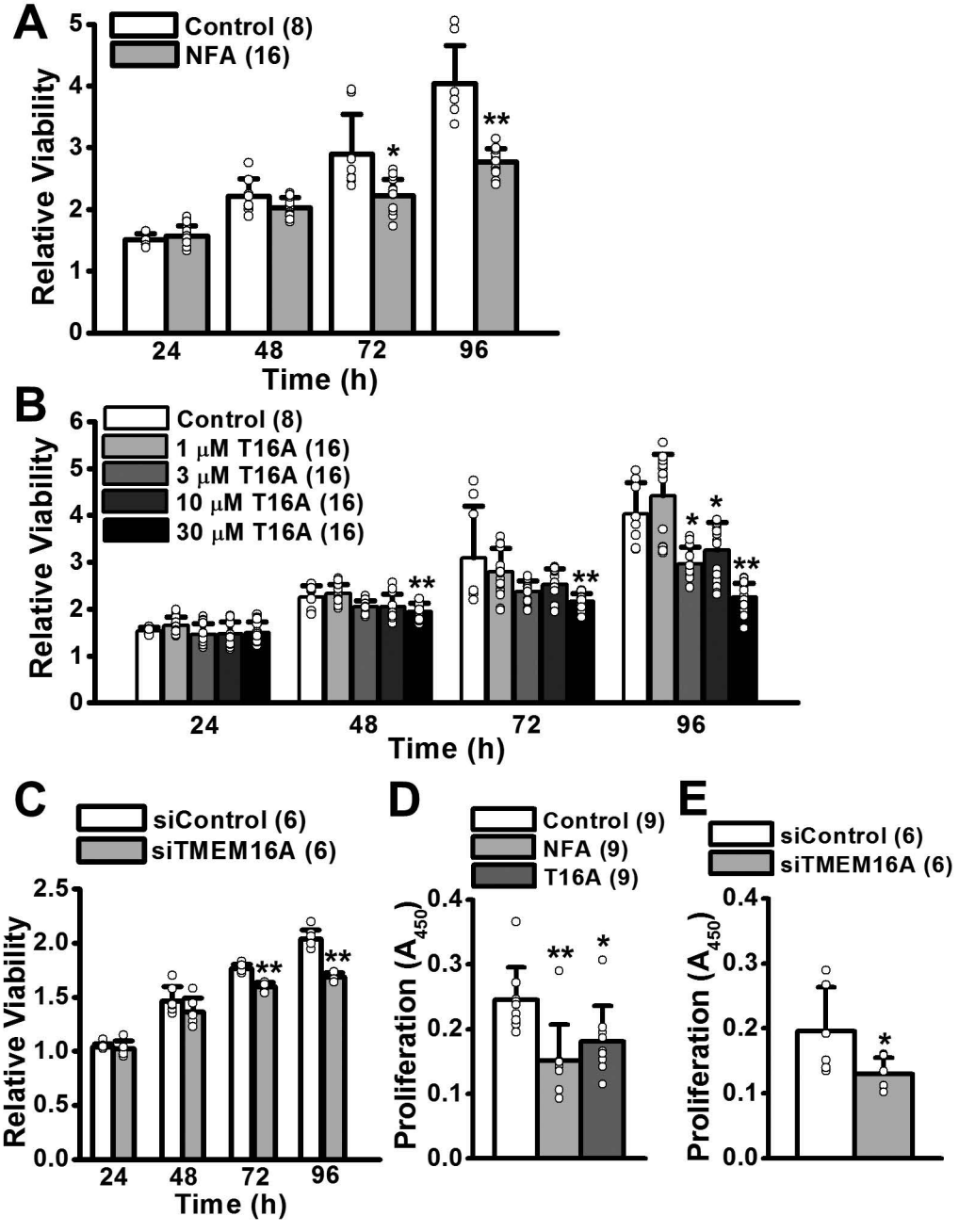
A
Control (8)
NFA (16)
Relative Viability
Time (h)
B
Control (8)
1 μM T16A (16)
3 μM T16A (16)
10 μM T16A (16)
30 μM T16A (16)
Relative Viability
Time (h)
C
siControl (6)
siTMEM16A (6)
Relative Viability
Time (h)
D
Control (9)
NFA (9)
T16A (9)
Proliferation (A450)
E
siControl (6)
siTMEM16A (6)
Proliferation (A450)

Figure 7

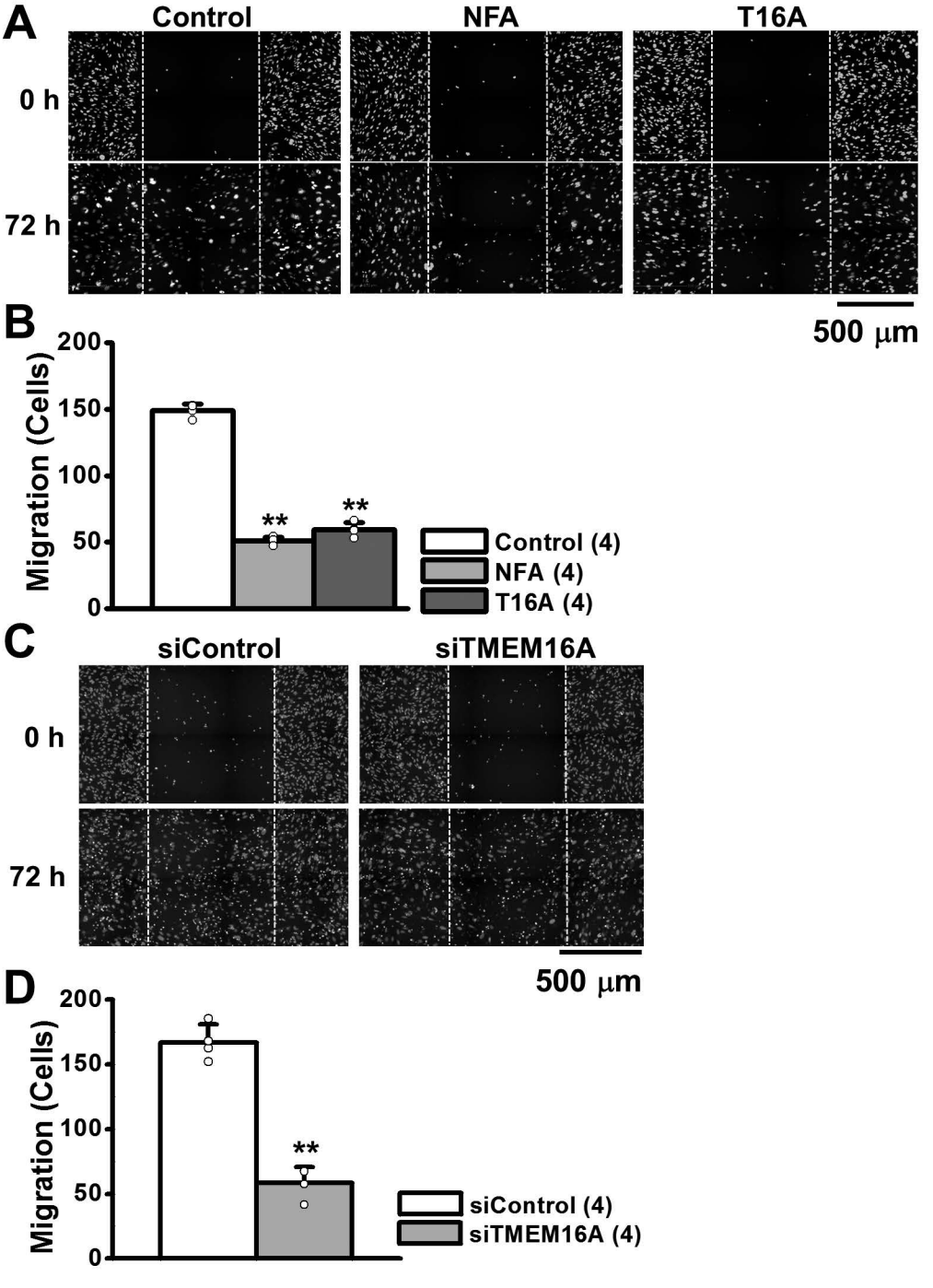
A
Control
NFA
T16A
0 h
72 h
500 μm
B
Migration (Cells)
200
150
100
50
0
**
**
Control (4)
NFA (4)
T16A (4)
C
siControl
siTMEM16A
0 h
72 h
500 μm
D
Migration (Cells)
200
150
100
50
0
**
siControl (4)
siTMEM16A (4)

Figure 8